Quantum mechanics and speed limit of ultrafast local control in spin chains

P. V. Pyshkin,[1,*] E. Ya. Sherman,[2,3] and Lian-Ao Wu[4,3]

[1]*Institute for Solid State Physics and Optics, Wigner Research Centre for Physics, P.O. Box 49, H-1525 Budapest, Hungary*

[2]*Department of Physical Chemistry, The University of the Basque Country UPV/EHU, 48080 Bilbao, Spain*

[3]*IKERBASQUE, Basque Foundation for Science, 48011 Bilbao, Spain*

[4]*Department of Theoretical Physics and History of Science, The University of the Basque Country UPV/EHU, 48080 Bilbao, Spain*

(Received 30 July 2019; published 2 December 2019)

We study optimization of fidelity for ultrafast transformation of a spin chain via external control of a local exchange coupling. We show that infidelity of such a process can be dramatically decreased by choosing a proper control profile in nonadiabatic time domain, predict main features of this profile analytically, corroborate them numerically with a gradient search algorithm, and discuss the corresponding quantum speed limit. For ultrafast transformations, the qualitative features of the obtained optimal control are system independent. Moreover, the main restrictions on its shape do not depend on the transformation time and remain valid up to the adiabatic limit. Our results can be applied to control a broad variety of quantum systems.

DOI: 10.1103/PhysRevA.100.063401

I. INTRODUCTION

Recent progress in experimental research on quantum systems described by moderate-size Hilbert spaces, such as ensembles of qubits, posed fascinating problems of optimal quantum control [1–5] of these systems. The quantum control aims at achieving desired quantum states or certain quantum operations with maximum possible fidelity using limited resources such as time or energy. The dynamics of quantum systems under external control can be unitary or nonunitary. The unitary dynamics is driven by a time-dependent controllable Hamiltonian $H(\mathbf{g}(t))$, where $\mathbf{g}(t)$ is a multicomponent control function. The controllable nonunitary dynamics is achievable by system measurements [6–10], via a controllable interaction with a non-Markovian environment [11–13] or via control of the unitary part of the evolution of open system [14].

We consider driving a quantum system from a ground state of initial Hamiltonian H_i to achieve at time T ground state of a final Hamiltonian H_f with $H(t) = H_i + g(t)(H_f - H_i)$, where $g(0) = 0$ and $g(T) = 1$. Although a high fidelity can be obtained by an adiabatic process [15] driven by a slowly varying $H(t)$ with, e.g., $g(t) = t/T$, this method requires a long evolution while optimized $g(t)$ can permit achieving a demanded quantum state for a relatively short T.

A possible approach to the quantum control, where the transitions occur between the ground states of $H(t)$, is based on the shortcut to adiabaticity [16–20]. However, this technique requires a control of all parts of a complex quantum system. Implementation of such a shortcut can be a part of quantum computation in arrays of quantum dots [21,22], or in quantum annealing [23], such as applied in D-Wave computer [24]. Here, by focusing on high fidelity ultrafast processes, we analytically obtain properties of optimal *local* control in the ultrashort time domain for a particular many-body system and corroborate our reasoning by a direct numerical optimization. We show that several properties of the finite time quantum control (even for the ultrashort time) can be explained by requiring a smooth passage to the adiabatic protocols, thus connecting these two limits. Although the reported results are obtained for spin chains, the proposed heuristic reasoning and numerical approach can be extended to a much broader class of quantum systems.

II. ULTRAFAST LOCAL CONTROL: THE PROBLEM SETTING

We concentrate on a local control acting only on a small part of a complex system, being a natural tool for cutting or stitching links between its parts, thus modifying its size and/or topology. We consider an Ising chain with N spins, as shown in Fig. 1, described by the Hamiltonian

$$H(g(t)) = J\sum_{n=1}^{N-1} X_n X_{n+1} + B\sum_{n=1}^{N} Z_n + g(t)JX_1X_N, \quad (1)$$

where X_k, Z_k are corresponding Pauli matrices of the kth spin and B is a magnetic field. It is useful to rewrite Hamiltonian (1) in a short form: $H(t) = H_0 + g(t)V$, where $V \equiv JX_1X_N$. We assume antiferromagnetic interaction and set $J = 1$. The last term in (1) connects the first and last spins in the chain. By assuming $g(0) = 0$ and $g(T) = 1$, we perform a transformation from an open to a ring-shaped chain via "stitching" a single link between the spins (see Fig. 1). Now we define initial and final Hamiltonians: $H_i \equiv H(g(0))$ and $H_f \equiv H(g(T))$. The corresponding ground states of these Hamiltonians are $|\varphi_i\rangle$ and $|\varphi_f\rangle$: $H_i|\varphi_i\rangle = \varepsilon_i|\varphi_i\rangle$ and $H_f|\varphi_f\rangle = \varepsilon_f|\varphi_f\rangle$. The state of the system during the evolution is $|\psi(t)\rangle = U(t)|\psi(0)\rangle$, where

$$U(t) = \mathcal{T}\exp\left(-i\int_0^t H(g(s))ds\right), \quad (2)$$

*pavel.pyshkin@gmail.com

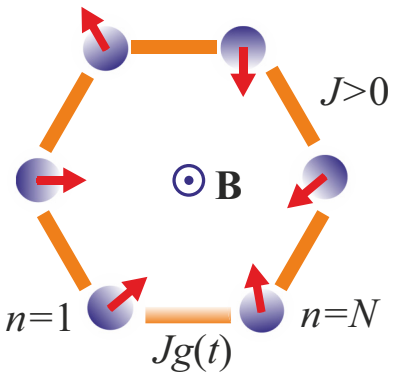

FIG. 1. Spin chain with one variable link strength in magnetic field $\mathbf{B} \parallel z$ axis.

$\mathcal{T}$ is the time-ordering operator, and we set $\hbar \equiv 1$ and the time unit as $1/J$. We assume that the initial state $|\psi(0)\rangle = |\varphi_i\rangle$ and study the controlled state-transition process with the following target fidelity f_T and infidelity R_T:

$$f_T \equiv |\langle\varphi_f|\psi(T)\rangle|, \quad R_T \equiv 1 - f_T. \tag{3}$$

Adiabatic theorem allows us to have an ideal state-transition protocol:

$$R_T \to 0, \quad \text{for } T \to \infty, \tag{4}$$

when $g(t) = t/T$. Note that the protocol (4) is valid only in the absence of level crossing for an arbitrary $g(t) \in (0, 1)$. In this work we assume that the evolution time belongs to one of three domains: ultrashort one ($T \ll 1$), short time ($T \sim 1$), and adiabatic one ($T \gg 1$), where the adiabatic theorem is valid. We will concentrate mainly on the physics of the optimal control in the ultrashort domain and analyze the general features being common for all three domains. Such ultrafast control can be achieved, e.g., by electrical manipulation of the bonds connecting quantum dots on the time scale much shorter than global change in the magnetic field strength [22].

If the ground state of H_i or H_f is degenerate we select $|\varphi_i\rangle$ or/and $|\varphi_f\rangle$ from some subspace. In such a case we assume that $|\varphi_i\rangle$ ($|\varphi_f\rangle$) is a nondegenerate ground state of Hamiltonian $H(\delta g)$ ($H(1-\delta g)$) for $\delta g \to +0$.

Our task is to find the optimal $g(t)$ to minimize the target infidelity functional $R_T[g(t)]$ for a *finite* time T. Note that our system (1) doesn't have complete controllability [25,26] because of locality of our control. Although the local control can, in general, be complete (see Ref. [27]), the Hamiltonian (1) doesn't satisfy assumptions made in Ref. [27] since iX_1X_N does not generate a Lie algebra in the subspace of first and Nth spins. Therefore, the result of our optimization is the minimal nonzero R_T.

In order to deal with a function instead of a functional we parametrize as follows:

$$g(\mathbf{a}, t) = \frac{t}{T} + a_1 \sin\left(\frac{\pi t}{T}\right) + a_2 \sin\left(\frac{2\pi t}{T}\right), \tag{5}$$

with $\mathbf{a} \equiv (a_1, a_2)$. Now the target infidelity is a function of two parameters $R_T = R_T(a_1, a_2)$. Parametrization (5) can be considered as a simple particular case of chopped-random-basis optimization [28,29]. Our task is to find optimal $\mathbf{a} = \mathbf{a}_{\text{opt}}$, with $R_T(\mathbf{a}_{\text{opt}}) = \min_{\mathbf{a}}\{R_T(\mathbf{a})\}$. Also we can rewrite statement (4) as $R_T \to 0$ for $T \to \infty$ and $\mathbf{a} \to \mathbf{0}$, and therefore we expect that $\mathbf{a} = \mathbf{0}$ is a good starting point for gradient numerical search.

III. OPTIMAL CONTROL FOR ULTRAFAST EVOLUTION

A. Analytical results for singular control parameters

It is possible to use the first two terms of a Dyson series for approximation of $U(T)$ when $T \to 0$. One can write

$$\begin{aligned} U(T) &\approx \exp(-iH_0T)[\mathbb{I} - iVG(T)] \\ &\approx [\mathbb{I} - iVG(T)]\exp(-iH_0T), \\ G(t) &= \int_0^t g(\mathbf{a}, s)ds, \end{aligned} \tag{6}$$

and $\mathbb{I}$ is the identity operator. By using $\langle\varphi_f|V|\varphi_i\rangle = \langle\varphi_f|H_f - H_i|\varphi_i\rangle = (\varepsilon_f - \varepsilon_i)f_0$, where $f_0 = \langle\varphi_f|\varphi_i\rangle$, we obtain that this approximation leads to a quadratic T dependence of the target fidelity

$$R_0 - R_T \approx |f_0|\alpha(\mathbf{a})T^2, \tag{7}$$

where $R_0 \equiv 1 - |f_0|$, and α is a coefficient, e.g., $\alpha(\mathbf{0}) = (\varepsilon_i - \varepsilon_f)^2/8$. The quadratic behavior with $dR_T/dT|_{T=0} = 0$ is an understandable feature of the sudden approximation [30], where the initial state remains almost intact after fast change in the Hamiltonian. However, Eq. (7) being valid only for $|\mathbf{a}| \ll T^{-1}$ provides an inefficient optimization and, therefore, one needs to go beyond this condition.

A more convenient way to go beyond the simple sudden approximation is to apply the following interaction picture:

$$U(T) \approx e^{-iVG(T)}\left(\mathbb{I} - i\int_0^T e^{iVG(t)}H_0e^{-iVG(t)}dt\right), \tag{8}$$

with the validity of the integral expression (8) being not explicitly related to the magnitude of $g(t)$. For $V \equiv X_1X_N$ we simplify matrix exponents in (8) as

$$e^{\pm iG(t)X_1X_N} = \mathbb{I}\cos G(t) \pm iX_1X_N \sin G(t). \tag{9}$$

Since only two terms, that is BZ_1 and BZ_N, in H_0 do not commute with $\exp[\pm iX_1X_NG(t)]$, by using algebra of Pauli matrices with $(X_1X_N)^2 = \mathbb{I}$, $X_kZ_kX_k = -Z_k$, and $Z_kX_k = -X_kZ_k = iY_k$, we simplify the integral in (8) as

$$\begin{aligned} &\int_0^T e^{iVG(t)}H_0e^{-iVG(t)}dt \\ &= \int_0^T [H_0 - B(Z_1 + Z_N) + B\,e^{iVG(t)}(Z_1 + Z_N)e^{-iVG(t)}]dt \\ &= [H_0 - B(Z_1 + Z_N)]T \\ &\quad + B(Z_1 + Z_N)\beta_T(\mathbf{a}) + B(Y_1X_N + X_1Y_N)\gamma_T(\mathbf{a}), \end{aligned} \tag{10}$$

where

$$\beta_T(\mathbf{a}) \equiv \int_0^T \cos[2G(t)]dt, \quad \gamma_T(\mathbf{a}) \equiv \int_0^T \sin[2G(t)]dt. \tag{11}$$

Now we analyze the integral terms in (10). If we assume the control is very weak when, for any given t, $G(t) \to 0$, we arrive at Eq. (7). The opposite case of a strong control should

be considered in more detail. To get insight into the evolution, we assume for the moment a pulsed control: $g(t) = g_1$, for $0 < t < T/2$ and $g(t) = g_2$, for $T/2 < t < T$. In this case we have $G(t) = g_1 t, t < T/2$. Part of the last integral in (10) can be written as

$$\int_0^{T/2} \sin(2g_1 t)dt = \frac{T}{2}(g_1 T)^{-1}[1 - \cos(g_1 T)], \qquad (12)$$

where we picked out linear proportionality on T as in the other terms in (10). Now we see that the contribution of this integral goes to zero in two limits: (1) $g_1 T \to 0$ and (2) $g_1 T \to \infty$. Thus we have reached an important conclusion that for effective control one must have $g_1 T = \text{const}$ for $T \to 0$. The same conclusion can be made for g_2 by analysis of the $T/2 < t < T$ interval.

As the next step in our reasoning we require that the optimal control enhances the fidelity, that is,

$$\lim_{T\to 0} |\langle\varphi_f|U_{\text{opt}}(T)|\varphi_i\rangle| \geqslant |\langle\varphi_f|\varphi_i\rangle|. \qquad (13)$$

In order to satisfy (13) we can require $\lim_{T\to 0} G(T) = 0$ for optimal control [see Eq. (8)]. This means that for two pulses one must have $g_{2\text{opt}} = -g_{1\text{opt}}$. All these conclusions now can be applied for smooth optimal control function (5) in the following way:

$$\lim_{T\to 0} a_{1\text{opt}} = C_1, \quad \lim_{T\to 0} a_{2\text{opt}} = \frac{C_2}{T}, \qquad (14)$$

where constants $C_{1,2}$ are to be obtained by numerical calculations based on Eq. (10).

Using result (10) we write the target infidelity as

$$R_0 - R_T \approx |f_0|B[(\beta_T(\mathbf{a}) - T)F_1 + \gamma_T(\mathbf{a})F_2], \qquad (15)$$

$$F_1 = \text{Im}\frac{f_Z f_0^*}{|f_0|^2}, \quad F_2 = \text{Im}\frac{f_{XY} f_0^*}{|f_0|^2}, \qquad (16)$$

where

$$f_Z = \langle\varphi_f|Z_1 + Z_N|\varphi_i\rangle\,, \quad f_{XY} = \langle\varphi_f|X_1 Y_N + Y_1 X_N|\varphi_i\rangle\,. \qquad (17)$$

Since, without loss of generality, we can assume that the states $|\varphi_i\rangle$ and $|\varphi_f\rangle$ are real, we obtain $F_1 = 0$, $\text{Re}F_2 = 0$ and thus our result does not depend on $\beta_T(\mathbf{a})$.

Expression (15) was derived using

$$\langle\varphi_f|U(T)|\varphi_i\rangle = \langle\varphi_f|\,[\mathbb{I} - iB(Z_1 + Z_N)[\beta_T(\mathbf{a}) - T] - iB(Y_1 X_N + X_1 Y_N)\gamma_T(\mathbf{a})]e^{-iH_0 T}\,|\varphi_i\rangle + O(T^2). \qquad (18)$$

Here we also assume $G(T) = 0$ for all values of T. This assumption means that we chose $a_1 = -\pi/4$ as the optimal value for any small nonzero T [31]. It is important that optimized function $\gamma_T(\mathbf{a}_{\text{opt}}) = K_\gamma T$ is linear for small T, where $\gamma_T(\mathbf{a}_{\text{opt}}) = \max_{\mathbf{a}}\{\gamma_T(\mathbf{a})\}$, K_γ is a system-dependent coefficient, and $\mathbf{a}_{\text{opt}}$ satisfies (14). Thus the linear approximation to optimal infidelity is

$$R_0 - R_T = |f_0|BK_\gamma F_2 T. \qquad (19)$$

Linearly decreasing behavior of infidelity (19) under optimal control gives a big advantage in comparison with quadratic (7) for short time T. The spatial symmetry of Hamiltonian (1) assures that F_2 is an odd function of B, corresponding to the fidelity independent of the direction of the magnetic field.

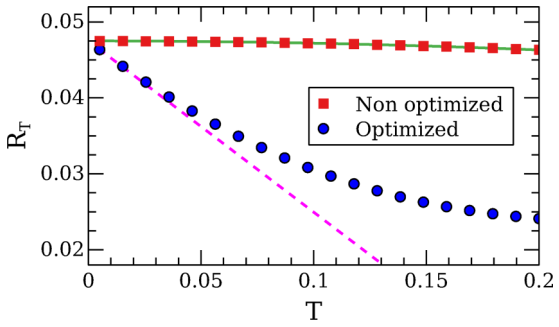

FIG. 2. Optimized and nonoptimized infidelity R_T for ultrashort timescale as a function of the process time T. The linear approximation (19) for optimized infidelity is given by the dashed line.

B. Numerical examples

To illustrate the above arguments, we study a chain with $N = 6$ spins and $B = 0.9$, and relate the results of direct numerical simulations to expressions (7), (15), and (19). Although the Ising chain in a transverse field is exactly solvable [32], we obtain the states $|\varphi_i\rangle$ and $|\varphi_f\rangle$ by direct numerical diagonalization of the corresponding Hamiltonians. Next, we use a gradient Broyden-Fletcher-Goldfarb-Shanno (BFGS) algorithm [33] in direct numerical search of $\mathbf{a}_{\text{opt}}(T)$. Exact numerical diagonalization was used in order to calculate $\mathbf{a}$-dependent propagators (2). In Fig. 2 we show nonoptimized $[g(t) = t/T]$ and optimized infidelities obtained by direct numerical simulations. To quantify linear approximation for the optimized fidelity, we first numerically obtain $f_0 = 0.9525$, $f_Z = -1.4090$, and $f_{XY} = 0.389i$, resulting in $F_1 = 0$, as expected, and $F_2 = 0.408$. It is easy to numerically find a maximum of a function $\gamma_T(\mathbf{a})$ for fixed T and $a_1 = -\pi/4$; the example of dependence $\gamma_T(a_2)$ for $T = 0.005$ is depicted in Fig. 3. From the last line of Table I we find $K_\gamma = 0.644$ and obtain $BK_\gamma F_2 = 0.237$. Additional numerical checks show that adding the next harmonic in (5) doesn't considerably change the optimal fidelity value. Note that expression (19) being linear in T is not linear in B since F_2 is B dependent.

In Fig. 4 (main panel) we show numerically optimized values of $a_{2\text{opt}}$, and approximation $a_2(T) = 3.24/T$, which

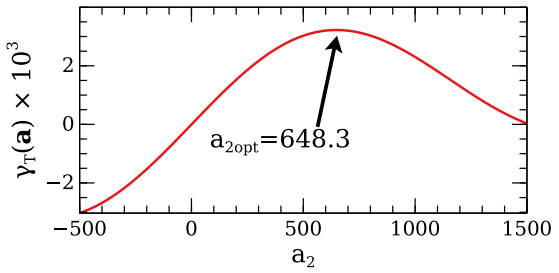

FIG. 3. Example of the dependence of $\gamma_T(\mathbf{a})$ function for fixed $T = 0.005$ and $a_1 = -\pi/4$. The optimal parameters from direct numerical BFGS optimization are $a_{1\text{opt}} = -0.9$ and $a_{2\text{opt}} = 646.8$.

TABLE I. Numerical evidence of linearity of $\gamma_T(\mathbf{a}_{\rm opt})$.

T	0.005	0.02	0.05	0.1
$a_{2\rm opt}$	648.3	162.4	65.2	32.84
$\gamma_T(\mathbf{a}_{\rm opt})$	0.00322	0.0129	0.0322	0.0642
$\gamma_T(\mathbf{a}_{\rm opt})/T$	0.644	0.644	0.643	0.642

follows from expression (14). The coefficient 3.24 can be obtained by taking product $Ta_{2\rm opt}$ from the first column of Table I. We see a good agreement between analytical and exact numerical optimization up to $T \approx 0.1$. In the inset of Fig. 4 we show numerically optimized values of $a_{1\rm opt}(T)$ and see that a_1 remains finite in the limit $T \to 0$ in agreement with (14), and thus our simplification $G(T) = 0$ for $T \to 0$ in (15) was rational. Note, in Fig. 4 we do not have $\lim_{T\to 0} a_{1\rm opt} = -\pi/4$ as we used in our analysis. However, the approximation we made is valid because $G(T) = T(1/2 + 2a_{1\rm opt}/\pi) \ll 1$ for any *finite* $|a_{1\rm opt}|$ and $T \to 0$.

Important input of (19) is that the optimal control parameters $\mathbf{a}_{\rm opt}$ can be evaluated from analysis of function $\gamma_T(\mathbf{a})$ (11), which, in turn, does not contain information about N and B. Therefore, we expect that the optimal control $g(t)$ for different quantum Ising chains is only very weakly system dependent in the ultrashort time limit. This *universality* is confirmed by Fig. 5(a), where we present the BFGS optimization results for chains with different parameters.

C. Relation to quantum speed limit

The optimal control (14) produces a strong perturbation, where the characteristic energy given by the time-energy uncertainty [34] is proportional to T^{-1}. Therefore, it is instructive to consider the quantum speed limit (QSL) time $T_{\rm QSL}$, that is, the minimal possible time required to transform the initial $|\varphi_i\rangle$ into the final $U_{\rm opt}(T)|\varphi_i\rangle$ state [35]. The $T_{\rm QSL}$ time is computed as [36]

$$\frac{T_{\rm QSL}}{T} = \frac{\arccos|\langle\varphi_i|U_{\rm opt}(T)|\varphi_i\rangle|}{\int_0^T |\langle\varphi_i|H(g(\mathbf{a}_{\rm opt},t))|\varphi_i\rangle|dt}, \tag{20}$$

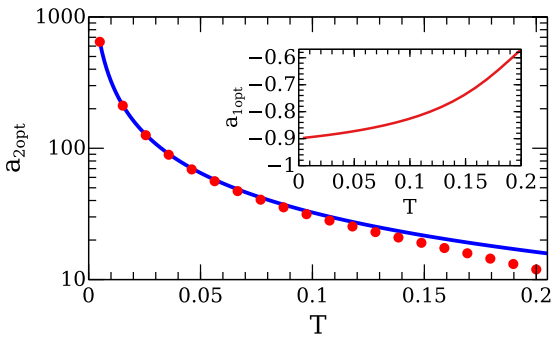

FIG. 4. Values of parameters for optimized control for ultrashort timescale as a function of the process time T. Red circles in the main panel and the solid line in the inset are the result of exact BFGS optimization; blue solid line in the main panel is analytical approximation $a_2(T) = 3.24/T$.

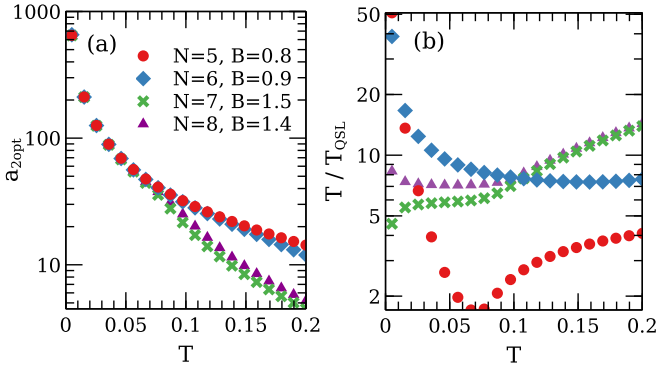

FIG. 5. (a) Optimal T-dependent control parameters for various values of N and B. This figure shows that in the limit $T \to 0$ they are almost the same for different spin chains and fields B. (b) The ratios $T/T_{\rm QSL}$ as functions of T for optimized evolution.

and the ratio $T/T_{\rm QSL}$ can be considered as the efficiency of the quantum control (see, e.g., Refs. [37,38]). In Fig. 5(b), where we show T dependence of $T/T_{\rm QSL}$, one can see the ratio $T/T_{\rm QSL} \gtrsim 5$, and this relatively large value can be related to the locality of the control.

IV. FROM ULTRAFAST TO ADIABATIC EVOLUTION

Here we briefly discuss features of optimal control when the evolution time T runs from ultrashort values to the adiabatic domain. In Fig. 6 we show nonoptimized and optimized infidelity for an extended interval of T. As can be seen, the nonoptimized infidelity goes to zero as a consequence of adiabaticity (4). Also, the maximal difference between optimized and nonoptimized infidelity appears at short time $T \lesssim 1$.

As we have shown in Ref. [39] the optimal shape of control function $g(t)$ is restricted by two requirements: (1) continuous transition from nonadiabatic to adiabatic time domain and (2) nonzero time derivative $\dot{g}(t)$ at $t = 0$ and $t = T$. These two assumptions lead to the following conditions:

$$\dot{g}(t \to 0) > 0, \quad \dot{g}(t \to T) > 0, \tag{21}$$

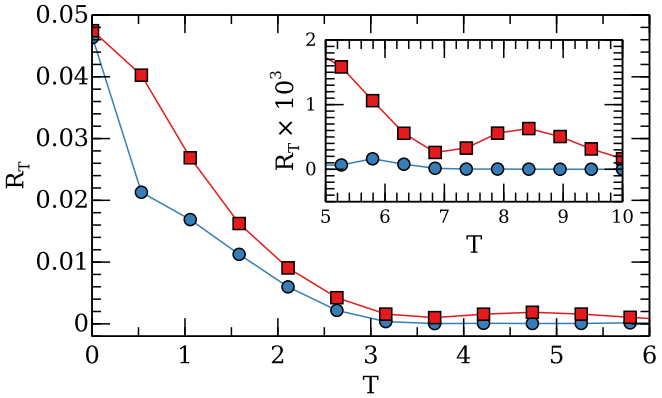

FIG. 6. Optimized (circles) and nonoptimized (squares) infidelities R_T for long timescale as function of the process time T.

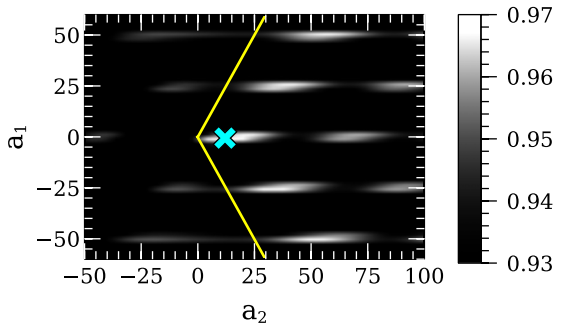

FIG. 7. Landscape of output fidelity as a function of a_1 and a_2 for $T = 0.2$. Yellow lines correspond to conditions (22) and cyan cross is the numerically obtained optimal value.

written in parametrization (5) as

$$-(1/\pi + 2a_2) < a_1 < 1/\pi + 2a_2. \tag{22}$$

Remarkably, the conditions (22) are T independent. It turns out that $\mathbf{a}_{\rm opt}$ from the numerical calculations satisfies (22) for ultrashort, short, and adiabatic processes, regardless of the time domain [this statement is as well T independent when we take more than two harmonics in (5)]. Note that first two harmonics in (5) provide the simplest efficient parametrization, which satisfies (21), for a strong energy pumping, with $|g(t)| \gg 1$ at a finite time interval.

In Fig. 7 we show the landscape of output fidelity as a function of $\mathbf{a}$ for $T = 0.2$. One can see that the high-fidelity "islands" form horizontal equidistant lines. Appearance of these lines is related to the possibility of the satisfaction of (13) by letting $U(T \to 0) = \mathbb{I}$ with $a_1 = \pi^2 l/2T$ ($\approx 24.7l$, $l = \pm 1, \pm 2, \ldots$) [see Eqs. (8) and (9)]. In comparison with the fidelity of different local maximums we see that initial point $\mathbf{a} = \mathbf{0}$ is the valid choice for a numerical BFGS search in order to avoid traps [40–44], and our assumption $\lim_{T\to 0} G(T) = 0$ is corroborated. Moreover, the universal initial point (0,0) [which satisfies (22)] for a numerical search connects together adiabatic and nonadiabatic time domains.

V. CONCLUSION

We demonstrated that properly designed incomplete local control can greatly decrease infidelity of unitary evolution in the nonadiabatic time domain, even for ultrafast transition processes. We presented an approximate analytical solution for finding the optimal control parameters in the ultrashort T domain and showed that optimization can lead to a linear in T decrease in the infidelity. Rather than achieving zero infidelity, this linearity is the main benefit of using the unrestricted energy resource in the case of incomplete local control.

The main features of the optimal control found by heuristic reasoning and analytical derivations have been confirmed by direct numerical simulations. Our results show that optimal control parameters for short T, being system independent, are somehow universal. Surprisingly, in our approach one needs to only analyze one of the extrema of a single-variable analytical function to find the optimal control parameters instead of the conventional numerical algorithm for computing propagators. We hope that our findings and approaches will be useful for further improvements of efficiency in realistic quantum control in a broad variety of systems.

ACKNOWLEDGMENTS

We gratefully acknowledge National Research, Development and Innovation Office of Hungary (Projects No. K124351 and No. 2017-1.2.1-NKP-2017-00001), the Basque Country Government (Grant No. IT472-10), the Spanish Ministry of Economy, Industry, and Competitiveness (MINECO), and the European Regional Development Fund FEDER Grant No. FIS2015-67161-P (MINECO/FEDER, UE).

[1] A. P. Peirce, M. A. Dahleh, and H. Rabitz, Phys. Rev. A **37**, 4950 (1988).
[2] C. Brif, R. Chakrabarti, and H. Rabitz, New J. Phys. **12**, 075008 (2010).
[3] A. Borzi, G. Ciaramella, and M. Sprengel, *Formulation and Numerical Solution of Quantum Control Problems (Computational Science & Engineering)* (SIAM–Society for Industrial & Applied Mathematics, Philadelphia, PA, 2017).
[4] T. Caneva, T. Calarco, R. Fazio, G. E. Santoro, and S. Montangero, Phys. Rev. A **84**, 012312 (2011).
[5] T. Caneva, A. Silva, R. Fazio, S. Lloyd, T. Calarco, and S. Montangero, Phys. Rev. A **89**, 042322 (2014).
[6] Y. Li, L.-A. Wu, Y.-D. Wang, and L.-P. Yang, Phys. Rev. B **84**, 094502 (2011).
[7] I. A. Luchnikov and S. N. Filippov, Phys. Rev. A **95**, 022113 (2017).
[8] L.-A. Wu, D. A. Lidar, and S. Schneider, Phys. Rev. A **70**, 032322 (2004).
[9] P. V. Pyshkin, E. Y. Sherman, D.-W. Luo, J. Q. You, and L.-A. Wu, Phys. Rev. B **94**, 134313 (2016).
[10] J. M. Torres, J. Z. Bernád, G. Alber, O. Kálmán, and T. Kiss, Phys. Rev. A **95**, 023828 (2017).
[11] F. Verstraete, M. M. Wolf, and J. I. Cirac, Nat. Phys. **5**, 633 (2009).
[12] J. Jing and T. Yu, Phys. Rev. Lett. **105**, 240403 (2010).
[13] D.-W. Luo, P. V. Pyshkin, C.-H. Lam, T. Yu, H.-Q. Lin, J. Q. You, and L.-A. Wu, Phys. Rev. A **92**, 062127 (2015).
[14] R. Schmidt, A. Negretti, J. Ankerhold, T. Calarco, and J. T. Stockburger, Phys. Rev. Lett. **107**, 130404 (2011).
[15] M. Born and V. Fock, Z. Phys. **51**, 165 (1928).
[16] E. Torrontegui, S. Ibáñez, S. Martínez-Garaot, M. Modugno, A. del Campo, D. Guéry-Odelin, A. Ruschhaupt, X. Chen, and J. G. Muga, *Advances in Atomic, Molecular, and Optical Physics* (Elsevier, Amsterdam, 2013), p. 117.
[17] D. Guéry-Odelin, A. Ruschhaupt, A. Kiely, E. Torrontegui, S. Martínez-Garaot, and J. G. Muga, Rev. Mod. Phys. **91**, 045001 (2019).
[18] M. Demirplak and S. A. Rice, J. Phys. Chem. A **107**, 9937 (2003).
[19] M. V. Berry, J. Phys. A: Math. Theor. **42**, 365303 (2009).

[20] F.-H. Ren, Z.-M. Wang, and Y.-J. Gu, Phys. Lett. A **381**, 70 (2017).
[21] D. Loss and D. P. DiVincenzo, Phys. Rev. A **57**, 120 (1998).
[22] G. Burkard, D. Loss, and D. P. DiVincenzo, Phys. Rev. B **59**, 2070 (1999).
[23] A. Das and B. K. Chakrabarti, Rev. Mod. Phys. **80**, 1061 (2008).
[24] C. C. McGeoch, *Adiabatic Quantum Computation and Quantum Annealing: Theory and Practice (Synthesis Lectures on Quantum Computing)* (Morgan & Claypool, London, 2014).
[25] S. G. Schirmer, A. I. Solomon, and J. V. Leahy, J. Phys. A: Math. Gen. **35**, 4125 (2002).
[26] V. Ramakrishna, M. V. Salapaka, M. Dahleh, H. Rabitz, and A. Peirce, Phys. Rev. A **51**, 960 (1995).
[27] D. Burgarth, S. Bose, C. Bruder, and V. Giovannetti, Phys. Rev. A **79**, 060305(R) (2009).
[28] T. Caneva, T. Calarco, and S. Montangero, Phys. Rev. A **84**, 022326 (2011).
[29] N. Rach, M. M. Müller, T. Calarco, and S. Montangero, Phys. Rev. A **92**, 062343 (2015).
[30] J. J. Sakurai and J. J. Napolitano, *Modern Quantum Mechanics*, 2nd ed. (Pearson, London, 2010).
[31] In other words, we change the real function $G(\mathbf{a}_{\rm opt}, T) = T/2 + 2a_{1\rm opt}T/\pi$ [which as we assume must have a property $\lim_{T\to 0} G(\mathbf{a}_{\rm opt}, T) = 0$] to a constant $G(\mathbf{a}_{\rm opt}, T) = 0$. Thus the factor $\exp[-iV G(T)] = \mathbb{I}$ in Eq. (7).
[32] P. Pfeuty, Ann. Phys. (NY) **57**, 79 (1970).
[33] R. Fletcher, *Practical Methods of Optimization*, 2nd ed. (Wiley, New York, 1988).
[34] L. Mandelstam and I. Tamm, in *Selected Papers*, edited by B. M. Bolotovskii, V. Y. Frenkel, and R. Peierls (Springer, Berlin, 1991), p. 115.
[35] N. Margolus and L. B. Levitin, Physica D **120**, 188 (1998).
[36] S. Deffner and E. Lutz, J. Phys. A: Math. Theor. **46**, 335302 (2013).
[37] M. Murphy, S. Montangero, V. Giovannetti, and T. Calarco, Phys. Rev. A **82**, 022318 (2010).
[38] T. Caneva, M. Murphy, T. Calarco, R. Fazio, S. Montangero, V. Giovannetti, and G. E. Santoro, Phys. Rev. Lett. **103**, 240501 (2009).
[39] P. V. Pyshkin, E. Y. Sherman, J. Q. You, and L.-A. Wu, New J. Phys. **20**, 105006 (2018); P. V. Pyshkin, E. Y. Sherman, and L.-A. Wu, Acta Phys. Pol. A **135**, 1198 (2019).
[40] H. A. Rabitz, M. M. Hsieh, and C. M. Rosenthal, Science **303**, 1998 (2004).
[41] T.-S. Ho and H. Rabitz, J. Photochem. Photobiol., A **180**, 226 (2006).
[42] A. N. Pechen and D. J. Tannor, Phys. Rev. Lett. **106**, 120402 (2011).
[43] D. V. Zhdanov and T. Seideman, Phys. Rev. A **92**, 052109 (2015).
[44] D. V. Zhdanov, J. Phys. A: Math. Theor. **51**, 508001 (2018).